

Analytical Methods

Accepted Manuscript



This is an *Accepted Manuscript*, which has been through the Royal Society of Chemistry peer review process and has been accepted for publication.

Accepted Manuscripts are published online shortly after acceptance, before technical editing, formatting and proof reading. Using this free service, authors can make their results available to the community, in citable form, before we publish the edited article. We will replace this *Accepted Manuscript* with the edited and formatted *Advance Article* as soon as it is available.

You can find more information about *Accepted Manuscripts* in the [Information for Authors](#).

Please note that technical editing may introduce minor changes to the text and/or graphics, which may alter content. The journal's standard [Terms & Conditions](#) and the [Ethical guidelines](#) still apply. In no event shall the Royal Society of Chemistry be held responsible for any errors or omissions in this *Accepted Manuscript* or any consequences arising from the use of any information it contains.

A fluorescent probe based on N-doped carbon dots for highly sensitive detection of Hg²⁺ in aqueous solution

Zhi-hao Gao¹, Zheng-zhong Lin^{1,2}, Xiao-mei Chen¹, Hui-ping Zhong¹, Zhi-yong Huang^{1,3†}

1. College of Food and Biological Engineering, Jimei University, Xiamen, 361021, China;
2. Fujian Provincial Key Laboratory of Food Microbiology and Enzyme Engineering, Xiamen, 361021, China;
3. Fujian Collaborative Innovation Center for Exploitation and Utilization of Marine Biological Resources, Xiamen, 361102, China.

Abstract

A facile and green hydrothermal method was developed for the preparation of highly luminescent nitrogen-doped carbon dots (NCDs) by using anhydrous citric acid and urea as carbon source and nitrogen source, respectively. The NCDs show good water-solubility and exhibit excitation-independent fluorescence behaviors at the excitation of 300-390 nm with a quantum yield of 42.5% at λ_{em} of 440 nm. Based on the fluorescence quenching strategy, the NCDs were successfully applied to the measurement of Hg²⁺ in tap and lake water samples with high sensitivity and excellent selectivity. The detection limit was 7.3 nmol L⁻¹ (3σ , $n = 9$), indicating its potential applications to the detection of trace Hg²⁺ in water samples.

Introduction

Mercury (Hg) is a persistent pollutant with high toxicity that can be easily bio-accumulated in human body through food-chain, which has raised serious health concerns for decades.^{1,2} Therefore, the development of detection methods for trace Hg²⁺ in aqueous solution with high sensitivity and selectivity is of great necessity. The conventional analytical techniques, including cold-vapor atomic

Corresponding author. Tel.: +86-592-6181912; fax: +86-592-6180470. E-mail address: zhyhuang@jmu.edu.cn

1
2
3
4 absorption spectrometry (CV-AAS),³ cold-vapor atomic fluorescence spectrometry (CV-AFS),⁴ and
5
6 inductively coupled plasma mass spectrometry (ICP-MS)⁵, have been extensively used for the
7
8 measurement of Hg²⁺. However, most of these methods require large-scale instruments and
9
10 sophisticated sample preparation, which restricts their practical applications in the routine
11
12 monitoring of Hg²⁺.⁶ Thus, it is still of a great challenge to develop a rapid and simple method for
13
14 the detection of trace Hg²⁺ in aqueous solutions.
15
16
17
18

19 In recent years, fluorescent carbon dots (FCDs) have gained growing interests in bioimaging,
20
21 biological labeling and sensing⁷⁻⁹ due to the advantages of good water-solubility, low-toxicity and
22
23 excellent optical properties. Since FCDs were first discovered in the purification procedures of
24
25 single-walled carbon nanotubes in 2004,¹⁰ a variety of preparation methods of FCDs have been
26
27 developed, including laser ablation,¹¹ ultrasonic,¹² microwave-assisted,¹³ electrochemical¹⁴ and
28
29 hydrothermal methods,¹⁵ in which hydrothermal synthesis strategy is considered as a simple, direct
30
31 and efficient way to obtain FCDs.¹⁶
32
33
34
35

36 Based on the fluorescence quenching strategy, FCDs have been used as biosensors for the
37
38 detection of heavy metals.¹⁸⁻²¹ For example, Dong et al.²² described a novel sensing system of
39
40 branched poly(ethylenimine) functioned carbon dots for Cu²⁺ detection with a detection limit of 6
41
42 nmol L⁻¹. Li et al.¹⁸ showed the first use of carbon dots obtained from carbon soot by lighting a
43
44 candle as a cheap, effective fluorescent sensing platform for Ag⁺ detection with high selectivity. Lu
45
46 et al.⁷ used pomelo peel as the carbon source to synthesize FCDs by hydrothermal method for the
47
48 detection of Hg²⁺, in which the sensing principle is presumably due to the formation of a stable
49
50 non-fluorescent complex between FCDs and Hg²⁺.²³
51
52
53
54
55

56 Herein, a facile and green method was developed for the synthesis of highly luminescent
57
58
59
60

1
2
3
4 nitrogen-doped carbon dots (NCDs) by one-pot hydrothermal method. The NCDs were further used
5
6 as a biosensor for the detection of Hg^{2+} in aqueous solution with high sensitivity.
7

8 9 **Experimental**

10 11 **Reagents and materials**

12
13
14 Anhydrous citric acid and urea were purchased from Sinopharm Chemical Reagent Co., Ltd
15
16 (Shanghai, China). HgCl_2 , $\text{CdCl}_2 \cdot 2.5\text{H}_2\text{O}$, $\text{CuSO}_4 \cdot 5\text{H}_2\text{O}$, $\text{Pb}(\text{NO}_3)_2$, ZnCl_2 , $\text{MnSO}_4 \cdot \text{H}_2\text{O}$,
17
18 $\text{MgSO}_4 \cdot 7\text{H}_2\text{O}$, $\text{NiCl}_2 \cdot 6\text{H}_2\text{O}$, $\text{K}_2\text{Cr}_2\text{O}_7$, $\text{SrCl}_2 \cdot 6\text{H}_2\text{O}$, CaCl_2 , $\text{FeCl}_3 \cdot 6\text{H}_2\text{O}$ and quinine sulfate were
19
20 purchased from Xilong Chemical Co., Ltd (Guangdong, China). The stock solution of Hg^{2+} (2.5
21
22 mmol L^{-1}) was prepared by dissolving HgCl_2 in ultra-pure water containing 1% (v/v) HCl. The
23
24 standard solution of Hg^{2+} (1000 mg L^{-1} , GSB 04-1729-2004) was purchased from National Center
25
26 of Analysis and Testing for Nonferrous Metals and Electronic Materials (Beijing, China). All
27
28 chemicals were of analytical grade, and were used without any further purification. The water used
29
30 in all the experiments was purified with TKA Ultra (18.2 $\text{M}\Omega \text{ cm}$, Germany).
31
32
33
34
35
36
37

38 39 **Apparatus**

40
41
42 The UV absorption spectra were recorded with a UV-2100 spectrophotometer (Beijing LabTech,
43
44 China). Fluorescence spectra were measured on a Varian Cary Eclipse fluorescence
45
46 spectrophotometer (South East Chemicals & Instruments Ltd., Hong Kong, China). The Fourier
47
48 transform infrared (FT-IR) spectra were measured on a Nicolet 380 FT-IR spectrometer (Thermo
49
50 Scientific, US). Transmission electron microscopy (TEM) images were recorded with a JEM-2100
51
52 microscope (JEOL, Japan) operating at an accelerating voltage of 200 kV. X-ray photoelectron
53
54 spectroscopic (XPS) measurement was performed with an Escalab 250Xi spectrometer (VG
55
56
57
58
59
60

Scientific, UK). An AFS-640 hydride generation atomic fluorescence spectrometer (HG-AFS) (Beijing Ruili Instrumental Co., China) was used for the measurement of Hg^{2+} in tap and lake water samples. The pH values were measured using a pH510 meter (EUTECH, Singapore).

Synthesis of NCDs

NCDs were synthesized according to a reported method with slight modification.²⁴ Briefly, 0.5 g of anhydrous citric acid and urea were dissolved in 10 mL of deionized water, and were transferred to a stainless-steel Teflon-lined vessel, followed by hydrothermal treatment at 160 °C for 4 h in an oven (DHG-9146A, Shanghai Jing Hong Laboratory Instrument Co., Ltd.). After the vessel cooled to room temperature naturally, the obtained black-green solution in vessel was precipitated with acetone thrice to provide the NCDs. After dried under vacuum, the as-prepared NCDs were re-dispersed in acetate buffer (10 mmol L⁻¹, pH 6.0) at a concentration of 45 g L⁻¹ for further characterization and application.

Quantum yield measurement

The quantum yield (QY) of the synthesized NCDs was calculated using quinine sulfate as reference. Quinine sulfate (QY = 0.54 at 360 nm) was dissolved in H₂SO₄ (0.1 mol·L⁻¹, refractive index (n) = 1.33), while the NCDs were dissolved in acetate buffer solution (pH 6.0, n = 1.33). Their fluorescence spectra were both recorded at an excitation wavelength of 360 nm. To minimize the re-absorption effects, the absorbance of both solutions was limited below 0.1 at 360 nm.²⁵ The quantum yield was calculated using the following equation:

$$Q_c = Q_s \times \frac{F_c \times A_s \times n_c^2}{F_s \times A_c \times n_s^2}$$

1
2
3
4 Where Q is the quantum yield, F is the integrated emission intensity, n is the refractive index of the
5
6 solvent, and A is the optical absorbance at 360 nm measured with a UV–Vis spectrophotometer. The
7
8 subscript “ s ” and “ c ” refer to quinine sulfate with known QY value and NCDs, respectively.
9

10 11 **Fluorescence detection of Hg^{2+}**

12
13
14 In a typical assay, 1.5 mL of NCDs ($1.2 \mu\text{g mL}^{-1}$) in acetate buffer solutions ($10 \text{ mmol}\cdot\text{L}^{-1}$, pH 6.0)
15
16 was mixed with 0.5 mL of Hg^{2+} at different concentrations in centrifugal tubes (2 mL). After
17
18 incubation for 2 min at room temperature, the mixed solutions were recorded for fluorescence
19
20 intensities at an excitation wavelength of 340 nm.
21
22
23
24

25 26 **Tests of selectivity and interferences**

27
28
29 The selectivity of NCDs was examined by mixing NCDs with different interference ions including
30
31 Cd^{2+} , Cu^{2+} , Pb^{2+} , Mn^{2+} , Mg^{2+} , Ni^{2+} , Cr^{6+} , Fe^{3+} , Sr^{2+} , Ca^{2+} and Zn^{2+} . The fluorescence intensities of
32
33 NCDs in the absence (F_0) and presence (F) of the interference ions were measured. The F/F_0 ratios
34
35 of the interference ions were compared with that of Hg^{2+} at the same metal concentrations (20.0
36
37 $\mu\text{mol L}^{-1}$). For the interference testes, the NCDs solutions were respectively mixed with each of the
38
39 interference ions, followed by the addition of equal dosage of Hg^{2+} at $10.0 \mu\text{mol L}^{-1}$. After
40
41 incubation for 2 min at room temperature, the solutions were measured for the fluorescence
42
43 intensities at λ_{em} of 440 nm ($\lambda_{\text{ex}} = 340 \text{ nm}$).
44
45
46
47
48
49

50 51 **Detection of Hg^{2+} in real samples**

52
53
54 The practicality of NCDs-based probe for the detection of Hg^{2+} in tap water and lake water samples
55
56 was respectively evaluated. The tap water was obtained from our laboratory and was analyzed
57
58
59
60

1
2
3
4 without any further pretreatment. Another two water samples collected from local lakes were
5
6 filtered through 0.22 μm nylon membrane before analysis. Each of the water samples was mixed
7
8 with NCDs for 2 min at room temperature. Then, the fluorescence quenching intensity at λ_{em} of 440
9
10 nm was measured. The recovery experiments were also carried out by spiking the water samples
11
12 with Hg^{2+} standards at three levels.
13
14
15
16
17

18 **Results and discussion**

21 **Synthesis of NCDs**

22
23
24
25 The NCDs-based probe was prepared by a facile one-step hydrothermal method. Citric acid and
26
27 urea were used as the carbon source and nitrogen source, respectively. Under the condition of high
28
29 temperature and high pressure, a polymer-like material was formed between citric acid and urea
30
31 through a condensation polymerization reaction, and was further carbonized to form NCDs.²⁶ For
32
33 the optimization of the performance of NCDs, several synthesis parameters such as temperature,
34
35 reaction time and the ratio between citric acid and urea were investigated. In a typical optimization,
36
37 the amount of anhydrous citric acid and the solvent volume were kept a constant value, 0.5g and
38
39 10mL respectively. The other synthetic conditions varied as follows: (a) the amounts of urea
40
41 (0.17-2.5 g); (b) reaction temperature (140-200 $^{\circ}\text{C}$); (c) reaction time (3-6 h). The optimization
42
43 results shown in Fig. S1 were described as follows: (a) a mass ratio of 1:1 between citric acid and
44
45 urea, (b) the reaction temperature of 160 $^{\circ}\text{C}$, (c) the reaction time of 4 hours.
46
47
48
49
50
51
52

53 **Characterization**

54
55
56
57 The as-prepared NCDs display clear green color and emit blue fluorescence under the illumination
58
59
60

1
2
3
4 of UV light at 365 nm. The fluorescent quantum yield is 42.5% using quinine sulfate (QY 54% in
5
6 0.1 mol L⁻¹ H₂SO₄, λ_{ex} = 360 nm) as the reference. It can be clearly seen in Fig. 1A that the NCDs
7
8 show two obvious absorption peaks at 235 nm and 340 nm. The absorption peak at 235 nm can be
9
10 ascribed to the typical π-π* transition of the aromatic sp² bond, while the absorption peak at 340 nm
11
12 is due to the n-π* transition of C=O or C-OH bond in the NCDs.^{27, 28} The fluorescence spectra (Fig.
13
14 1B) indicate that the optimal excitation and emission wavelengths of NCDs were 340 nm and 440
15
16 nm, respectively. It should be noted that neither citric acid nor urea solution emits luminescence in
17
18 visible region at λ_{ex} of 340 nm, revealing that the bright blue fluorescence originates from NCDs.
19
20 The maximum emission wavelength (λ_{em}) of NCDs at 440 nm remains unchanged with the
21
22 excitation wavelengths increasing from 300 to 390 nm, and the highest fluorescence intensity
23
24 appears at λ_{ex} of 340 nm (Fig. 1C). The excitation-independent photoluminescence behavior might
25
26 be attributed to the less surface defects and the narrow particle size distributions of NCDs.^{29, 30}

27
28
29
30
31
32
33
34 Fig. 2B shows the FT-IR spectra of the as-prepared NCDs. The peak at 3430 cm⁻¹ is attributed
35
36 to the stretching vibrations of O-H and N-H, and the peak at 3170 cm⁻¹ corresponds to the
37
38 stretching vibration of C=C-H.³¹ The peaks around 2920 and 1660 cm⁻¹ are accordance with the
39
40 vibrations of C-H and C=O bonds, respectively.^{24, 32} Two characteristic peaks at 1600 cm⁻¹ and
41
42 1400 cm⁻¹ can be attributed to the asymmetric and symmetric stretching vibration of COO⁻,
43
44 respectively.⁷ The results reveal that the NCDs are functioned with plentiful hydrophilic groups
45
46 such as hydroxyl, carboxyl and amino groups, which endows the NCDs with favorable water
47
48 solubility.
49
50
51
52

53
54 The morphologies of NCDs characterized by TEM are shown in Fig. 2B. The TEM images
55
56 illustrate that the NCD particles are spherical and well dispersed without apparent aggregation with
57
58
59
60

1
2
3
4 an average diameter about 2.4 nm. The surface composition and elemental analysis of the NCDs
5
6 were characterized by XPS. The peaks at 284.8, 400.2 and 531.5 eV in a full scan XPS spectrum
7
8 (Fig. 3A) can be attributed to C1s, N1s, and O1s, respectively.³³ And the mass percentages of C, N
9
10 and O of the NCDs are 51.25%, 14.5% and 34.25%, respectively. In the high-resolution region of
11
12 C1s as shown in Fig. 3B, there are three peaks at 284.8, 286.8 and 288.4 eV which are attributed to
13
14 C-C/C=C, C-N and C=O groups, respectively.^{7, 13, 32, 34} The two peaks of the O1s spectrum (Fig. 3C)
15
16 at 531.2 and 532.7 eV are assigned to the C=O and C-OH/C-O-C groups, respectively,^{13, 19} while
17
18 the spectrum of N1s (Fig. 3D) shows three peaks at 399.4, 400.3 and 401.5 eV, which are attributed
19
20 to C-N-C, N-(C)₃- and N-H groups, respectively.^{7, 13, 16} In conclusion, the FT-IR and XPS spectra
21
22 confirm that the surfaces of the NCDs have been functionalized with multiple groups containing
23
24 oxygen and nitrogen atoms.
25
26
27
28
29
30
31

32 **Fluorescence stability of the NCDs**

33
34
35
36 The fluorescence intensities of the NCDs solutions under various conditions (low pH, high ionic
37
38 strengths and longtime illumination) were measured to investigate the stability. Result in Fig. 4A
39
40 shows that the fluorescence intensity of the NCDs is pH-dependent, in which the fluorescence
41
42 intensities increase with pH from 3.0 to 6.0, but keep unchanged above pH 6.0. Therefore, pH 6.0
43
44 was chosen for the subsequent experiments. Result in Fig. 4B shows that the fluorescence
45
46 intensities of NCDs keep constant at NaCl concentrations from 0.2 to 0.6 mol L⁻¹, followed by
47
48 slight decreases above 0.8 mol L⁻¹, indicating a high stability of the NCDs under high ionic strength
49
50 environment. This behavior is favorable for the potential application in biological labeling and
51
52 analytical detection. Moreover, the NCDs are found to present a high resistance of photobleaching
53
54
55
56
57
58
59
60

1
2
3
4 at continuous UV illumination (365 nm) as long as 1 h as shown in Fig. 4C, which may be a
5
6 consequence of the chemical structure of the NCDs with no graphite lattices.³² Result in Fig. 4D
7
8 shows that the NCDs exhibit stable emission in that they only lose about 3% of fluorescence after
9
10 storage at -4 °C for three weeks.

14 **Selectivity of the NCDs probe for Hg²⁺ detection**

17
18 Selectivity is an important parameter to evaluate the performance of NCDs as a fluorescent probe
19
20 for Hg²⁺ detection. Therefore, the fluorescence intensities of NCDs were respectively analyzed in
21
22 the presence of various metal ions including Hg²⁺, Cd²⁺, Cu²⁺, Pb²⁺, Mn²⁺, Mg²⁺, Ni²⁺, Cr⁶⁺, Fe³⁺,
23
24 Sr²⁺, Ca²⁺ and Zn²⁺ at the same concentrations. Results in Fig. 5A show that the addition of metal
25
26 ions causes slight decrease of fluorescence intensities except for Hg²⁺ that induces strong
27
28 fluorescence quenching of NCDs immediately. Meanwhile, the results of interference testes as
29
30 shown in Fig. 5B indicate that the addition of Hg²⁺ induces obvious fluorescence quenching even in
31
32 the presence of each interference metal ion, indicating that these metal ions do not interfere with the
33
34 detection of Hg²⁺ except for Cr⁶⁺ and Fe³⁺. With a large ionic radius and a special electronic layer
35
36 structure, Hg²⁺ is prone to be polarized and deformed by the coordinating atoms of O and N on the
37
38 surface of NCDs, thus forming stable NCDs-Hg²⁺ complexes through partial covalent bonds, which
39
40 might be the main reason for the outstanding selectivity and specificity of NCDs to Hg²⁺.¹³ As a
41
42 strong electron acceptor to the NCDs,³⁵ Hg²⁺ has stronger affinity to carboxylic, hydroxyl and
43
44 amino groups on the surface of the NCDs than the other metal ions.¹³ Furthermore, NCDs-Hg²⁺
45
46 complexes may facilitate charge transfer and restrain the radiative recombination of excitons,
47
48 leading to the significant fluorescence quenching effects.¹⁴
49
50
51
52
53
54
55
56
57
58
59
60

Optimization of the Hg^{2+} detection conditions

Experimental conditions such as buffer compositions, NCDs concentrations and incubation time were optimized based on detection sensitivity and accuracy. Results in Fig. S2A show that the buffer compositions at pH 6.0 almost do not affect the initial fluorescence intensities of NCDs, but present obvious effects on the fluorescence quenching after the addition of Hg^{2+} . Therefore, acetate buffer (10 mmol L^{-1}) with pH 6.0 was chosen as the aqueous medium for Hg^{2+} detection.

NCDs at different concentrations present a sensitive measurement for Hg^{2+} by quenching effect. As shown in Fig. S2B, $1.2 \mu\text{g mL}^{-1}$ of NCDs is found to present the highest quenching efficiency ($F/F_0 = 0.81$) for $1 \mu\text{mol L}^{-1}$ of Hg^{2+} . The result shows that the fluorophore at very low concentration can't be effectively quenched by Hg^{2+} , similarly, for a given concentration of Hg^{2+} the quenching efficiency decreases at the high concentrations of fluorophore. It has been found that the lower concentration of fluorophore, the larger the change of F/F_0 value.³⁶ Therefore, $1.2 \mu\text{g mL}^{-1}$ of NCDs was chosen in the present study. The results in Fig. S2C show the dependence of incubation time on the fluorescence quenching. It costs 80 seconds only to reach quenching equilibrium, indicating that the quenching rate is fairly fast.

Linear range

To evaluate the sensitivity of this system, Hg^{2+} standard solutions with different concentrations were mixed with the NCDs under the optimized conditions. As shown in Fig. 6A, the fluorescence intensity of the NCDs is sensitive to the concentration of Hg^{2+} . Fig. 6B clearly shows the calibration curve of F/F_0 versus the concentrations of Hg^{2+} ions. The inset plot of Fig. 6B indicates a good linear correlation ($R^2 = 0.9992$) can be obtained with the concentrations of Hg^{2+} ranging from 0.05

1
2
3
4 $\mu\text{mol L}^{-1}$ to $5 \mu\text{mol L}^{-1}$.
5
6

7 **Hg²⁺ measurement in real samples**

8
9

10 One tap water and two lake water samples were used for the Hg²⁺ measurement by the NCDs
11 fluorescent probe together with HG-AFS to verify the accuracy and reliability of the analytical
12 procedure. The results listed in Table 1 show that the analytical data of the NCDs fluorescent probe
13 method is in accordance with the verification values of HG-AFS method. The detection limit of the
14 NCDs fluorescent probe method is 7.3 nmol L^{-1} (3σ , $n = 9$), which is comparable to the previous
15 reports (Table 2), especially much lower than that of the NCDs fluorescent probe for Hg²⁺ detection
16 ³⁸, and may be due to the different sources of carbon and nitrogen used and the different synthesis
17 conditions compared with these previous NCDs preparation. In addition, it was found that humic
18 acid with concentration ranging from $1\text{-}100 \mu\text{mol L}^{-1}$ in water does not interfere with the fluorescent
19 quenching efficiency of Hg²⁺ as shown in Fig. S3. Because the detection limit is also lower than the
20 maximum permitted value (10 nmol L^{-1}) of mercury in drinking water
21 (Environmental Protection Agency of the United States),¹³ the developed NCDs-based sensor
22 presents a promising sensing platform for the detection of Hg²⁺ in freshwater including drinking
23 water.
24
25
26
27
28
29
30
31
32
33
34
35
36
37
38
39
40
41
42
43
44
45

46 **Conclusion**

47
48
49

50 In summary, the highly luminescent N-doped carbon dots (NCDs) were synthesized by a facile
51 one-step hydrothermal method with anhydrous citric acid and urea as carbon source and nitrogen
52 source, respectively. The as-prepared NCDs, with a quantum yield of 42.5%, exhibit outstanding
53
54
55
56
57
58
59
60

1
2
3
4 selectivity and sensitivity of fluorescence quenching for Hg^{2+} and can be served as an effective
5
6 fluorescent sensing probe for quantitative detection of trace Hg^{2+} in aqueous solutions with a
7
8 detection limit of 7.3 nmol L^{-1} .
9

10 11 **Acknowledgements**

12
13
14 This work was supported by the Science and Technology Planning Project of Fujian Province,
15
16 China (2012Y0052, 2014Y0045); the Science and Technology Planning Project of Xiamen, China
17
18 (3502Z20143018); Fujian Provincial Key Laboratory of Food Microbiology and Enzyme
19
20 Engineering (M20140902); the Foundation for Innovative Research Team of Jimei University,
21
22 China (2010A007); National Undergraduate Training Programs for Innovation and
23
24 Entrepreneurship (201410390009, 20141039047).
25
26
27
28
29

30 31 **References:**

- 32 1 A. Renzoni, F. Zino and E. Franchi, *Environ. Res.*, 1998, **77**, 68-72.
- 33 2 H. Tao, T. Hu, J. Yan and J. Di, *Sens. Actuators, B*, 2015, **208**, 43-49.
- 34 3 N. Pourreza and K. Ghanemi, *J. Hazard. Mater.*, 2009, **161**, 982-987.
- 35 4 M. J. Campbell, G. Vermeir, R. Dams and P. Quevauviller, *J. Anal. Atom. Spectrom.*, 1992, **7**, 617-621.
- 36 5 Y. Li, C. Chen, B. Li, J. Sun, J. Wang, Y. Gao, Y. Zhao and Z. Chai, *J. Anal. At. Spectrom.*, 2006, **21**, 94-96.
- 37 6 M. Leermakers, W. Baeyens, P. Quevauviller and M. Horvat, *TrAC, Trends Anal. Chem.*, 2005, **24**, 383-393.
- 38 7 W. Lu, X. Qin, S. Liu, G. Chang, Y. Zhang, Y. Luo, A. M. Asiri, A. O. Al-Youbi and X. Sun, *Anal. Chem.*,
39 2012, **84**, 5351-5357.
- 40 8 L. Cao, X. Wang, M. J. Meziani, F. Lu, H. Wang, P. G. Luo, Y. Lin, B. A. Harruff, L. M. Veca, D. Murray, S.
41 Xie and Y. Sun, *J. Am. Chem. Soc.*, 2007, **129**, 11318-11319.
- 42 9 C. C. Fu, H. Y. Lee, K. Chen, T. S. Lim, H. Y. Wu, P. K. Lin, P. K. Wei, P. H. Tsao, H. C. Chang and W.
43 Fann, *Proc. Natl. Acad. Sci. (USA)*, 2007, **104**, 727-732.
- 44 10 X. Xu, R. Ray, Y. Gu, H. J. Ploehn, L. Gearheart, K. Raker and W. A. Scrivens, *J. Am. Chem. Soc.*, 2004,
45
46
47
48
49
50
51
52
53
54
55
56
57
58
59
60
126, 12736-12737.

- 1
2
3
4
5
6
7
8
9
10
11
12
13
14
15
16
17
18
19
20
21
22
23
24
25
26
27
28
29
30
31
32
33
34
35
36
37
38
39
40
41
42
43
44
45
46
47
48
49
50
51
52
53
54
55
56
57
58
59
60
- 11 H. M. R. Gonçalves, A. J. Duarte and J. C. G. Esteves Da Silva, *Biosens. Bioelectron.*, 2010, **26**, 1302-1306.
- 12 H. Li, X. He, Y. Liu, H. Huang, S. Lian, S. Lee and Z. Kang, *Carbon*, 2011, **49**, 605-609.
- 13 X. Qin, W. Lu, A. M. Asiri, A. O. Al-Youbi and X. Sun, *Sens. Actuators, B*, 2013, **184**, 156-162.
- 14 Y. Zhang, L. Wang, H. Zhang, Y. Liu, H. Wang, Z. Kang and S. Lee, *RSC Adv.*, 2013, **3**, 3733-3738.
- 15 J. Gu, W. Wang, Q. Zhang, Z. Meng, X. Jia and K. Xi, *RSC Adv.*, 2013, **3**, 15589-15591.
- 16 H. Huang, J. Lv, D. Zhou, N. Bao, Y. Xu, A. Wang and J. Feng, *RSC Adv.*, 2013, **3**, 21691-21696.
- 17 S. N. Baker and G. A. Baker, *Angew. Chem. Int. Ed.*, 2010, **49**, 6726-6744.
- 18 H. Li, J. Zhai and X. Sun, *Langmuir*, 2011, **27**, 4305-4308.
- 19 S. Liu, J. Tian, L. Wang, Y. Zhang, X. Qin, Y. Luo, A. M. Asiri, A. O. Al Youbi and X. Sun, *Adv. Mater.*, 2012, **24**, 2037-2041.
- 20 L. Zhou, Y. Lin, Z. Huang, J. Ren and X. Qu, *Chem. Commun.*, 2012, **48**, 1147-1149.
- 21 S. Qu, H. Chen, X. Zheng, J. Cao and X. Liu, *Nanoscale*, 2013, **5**, 5514-5518.
- 22 Y. Dong, R. Wang, G. Li, C. Chen, Y. Chi and G. Chen, *Anal. Chem.*, 2012, **84**, 6220-6224.
- 23 S. Y. Lim, W. Shen and Z. Gao, *Chem. Soc. Rev.*, 2015, **44**, 362-381.
- 24 Y. Hou, Q. Lu, J. Deng, H. Li and Y. Zhang, *Anal. Chim. Acta*, 2015, **866**, 69-74.
- 25 S. Dhami, A. J. De Mello, G. Rumbles, S. M. Bishop, D. Phillips and A. Beeby, *Photochem. Photobiol.*, 1995, **61**, 341-346.
- 26 Y. Zhang, Y. H. He, P. P. Cui, X. T. Feng, L. Chen, Y. Z. Yang and X. G. Liu, *RSC Adv.*, 2015, **5**, 40393-40401.
- 27 W. W. Liu, Y. Q. Feng, X. B. Yan, J. T. Chen and Q. J. Xue, *Adv. Funct. Mater.*, 2013, **23**, 4111-4122.
- 28 L. Han, F. Wang, Y. Wang, J. Ye, W. Qiu, H. Zhang, X. Gao, Z. Gong and X. Gu, *Eur. J. Med. Genet.*, 2014, **57**, 571-575.
- 29 Z. Yang, M. Xu, Y. Liu, F. He, F. Gao, Y. Su, H. Wei and Y. Zhang, *Nanoscale*, 2014, **6**, 1890-1895.
- 30 Z. Li, H. Yu, T. Bian, Y. Zhao, C. Zhou, L. Shang, Y. Liu, L. Wu, C. Tung and T. Zhang, *J. Mater. Chem. C.*, 2015, **3**, 1922-1928.
- 31 J. Hou, J. Li, J. Sun, S. Ai and M. Wang, *RSC Adv.*, 2014, **4**, 37342-37348.
- 32 S. Zhu, Q. Meng, L. Wang, J. Zhang, Y. Song, H. Jin, K. Zhang, H. Sun, H. Wang and B. Yang, *Angew. Chem.*, 2013, **125**, 4045-4049.
- 33 Y. Zhang, D. Ma, Y. Zhuang, X. Zhang, W. Chen, L. Hong, Q. Yan, K. Yu and S. Huang, *J. Mater. Chem.*, 2012, **22**, 16714-16718.

- 1
2
3
4 34 J. Wang, C. F. Wang and S. Chen, *Angew. Chem.*, 2012, **124**, 9431-9435.
5
6 35 Y. Liu, C. Liu and Z. Zhang, *Appl. Surf. Sci.*, 2012, **263**, 481-485.
7
8 36 X. Luo, L. Qiang, J. Qin and Z. Li, *ACS Appl. Mater. Inter.*, 2009, **11**, 2529-2535
9
10 37 Y. Guo, Z. Wang, H. Shao and X. Jiang, *Carbon*, 2013, **52**, 583-589.
11
12 38 R. Zhang and W. Chen, *Biosens. Bioelectron.*, 2014, **55**, 83-90.
13
14 39 C. Guo and J. Irudayaraj, *Anal. Chem.*, 2011, **8**, 2883-2889.
15
16 40 X. Cui, L. Zhu, J. Wu, Y. Hou, P. Wang, Z. Wang and M. Yang, *Biosens. Bioelectron.*, 2015, **63**, 506-512.
17
18 41 L. Li, B. Yu and T. You, *Biosens. Bioelectron.*, 2015, **74**, 263-269.
19
20
21
22
23
24
25
26
27
28
29
30
31
32
33
34
35
36
37
38
39
40
41
42
43
44
45
46
47
48
49
50
51
52
53
54
55
56
57
58
59
60

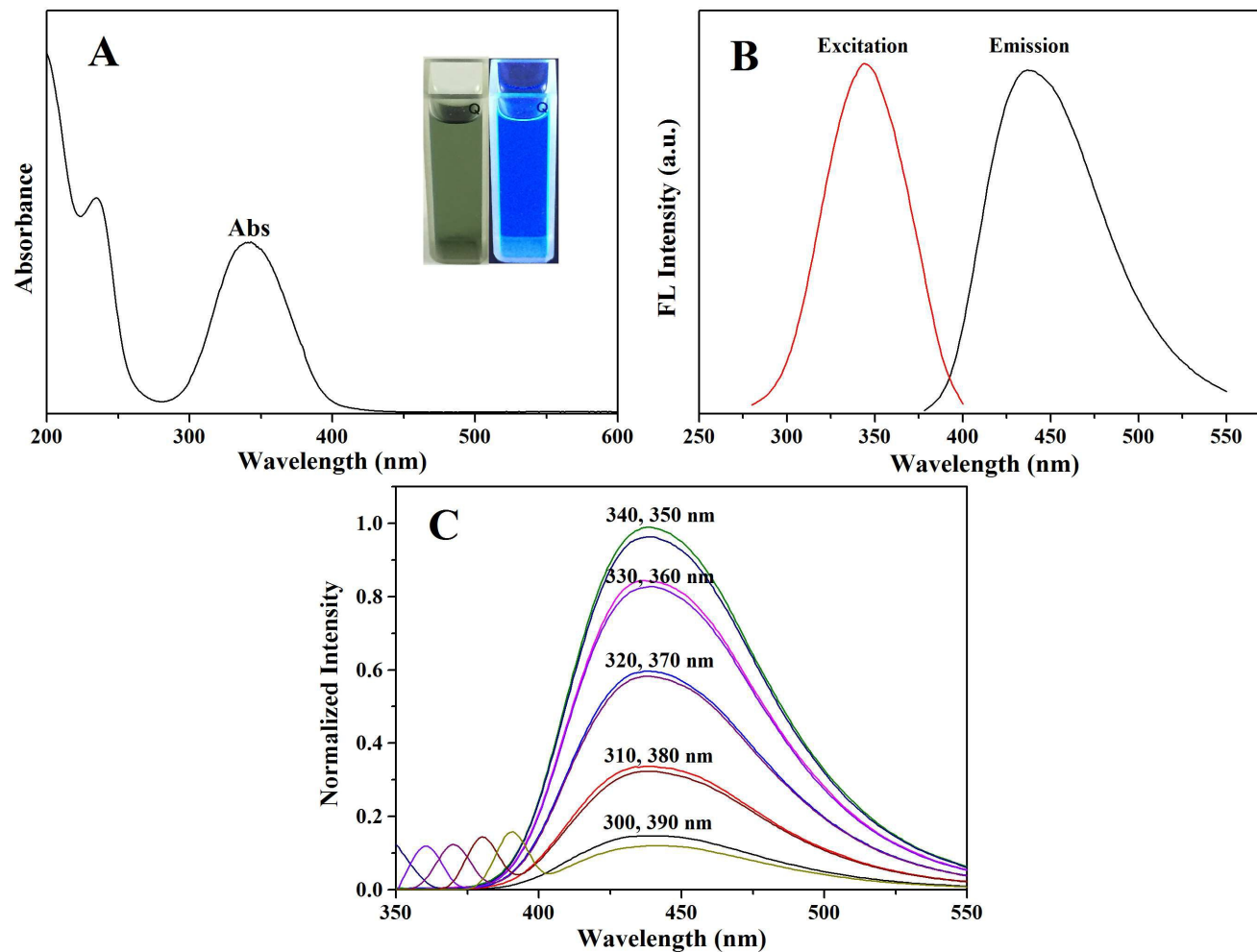


Fig. 1. (A) UV-vis absorption spectrum of the NCDs. Inset shows the colors of the NCD aqueous solution under visible light (left) and UV light (right). (B) Fluorescence excitation and emission spectra of the NCDs. (C) Emission spectra of the NCDs at different excitation wavelengths from 300 to 390 nm.

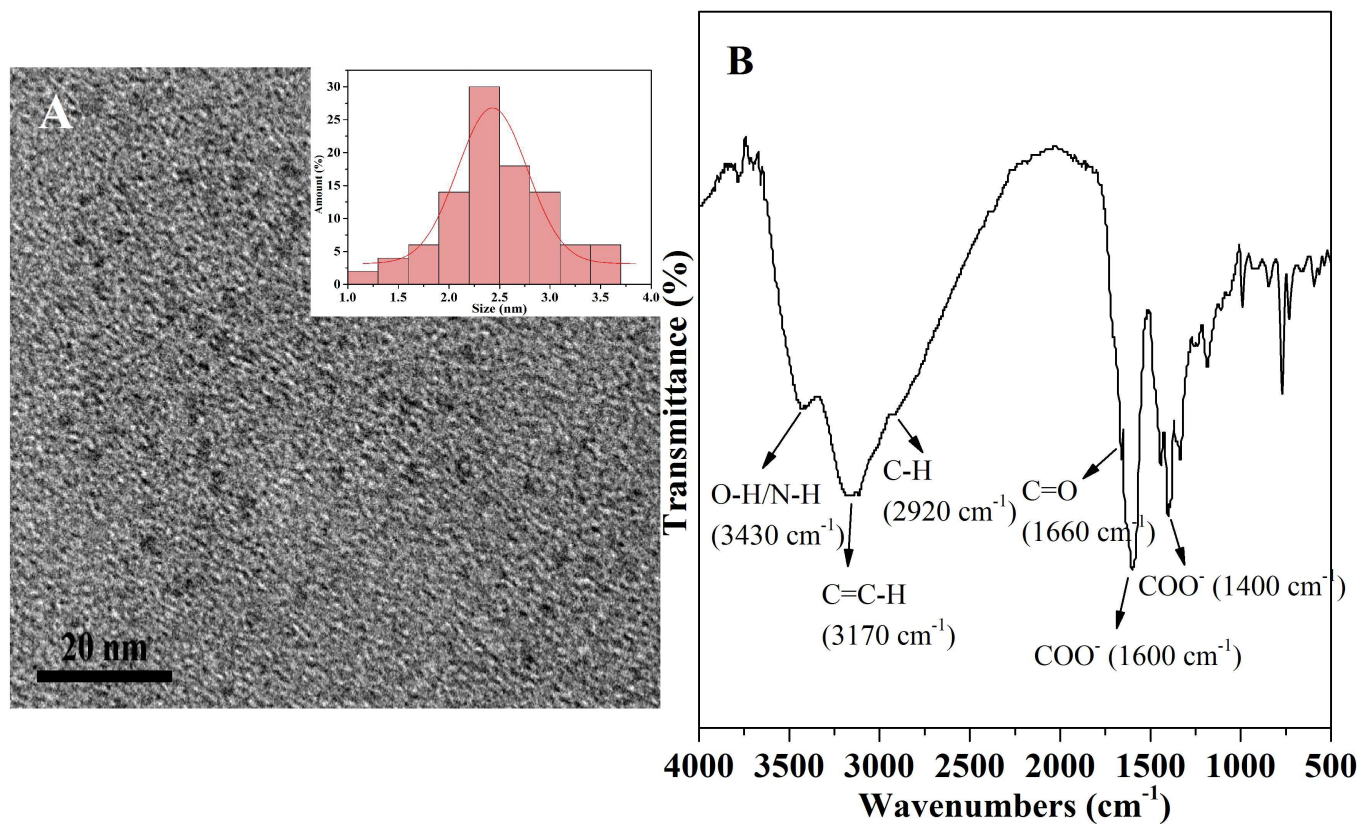


Fig. 2. (A) TEM image of the NCD particles. Inset shows the distribution of particle sizes. (B) FT-IR spectrum of the NCDs.

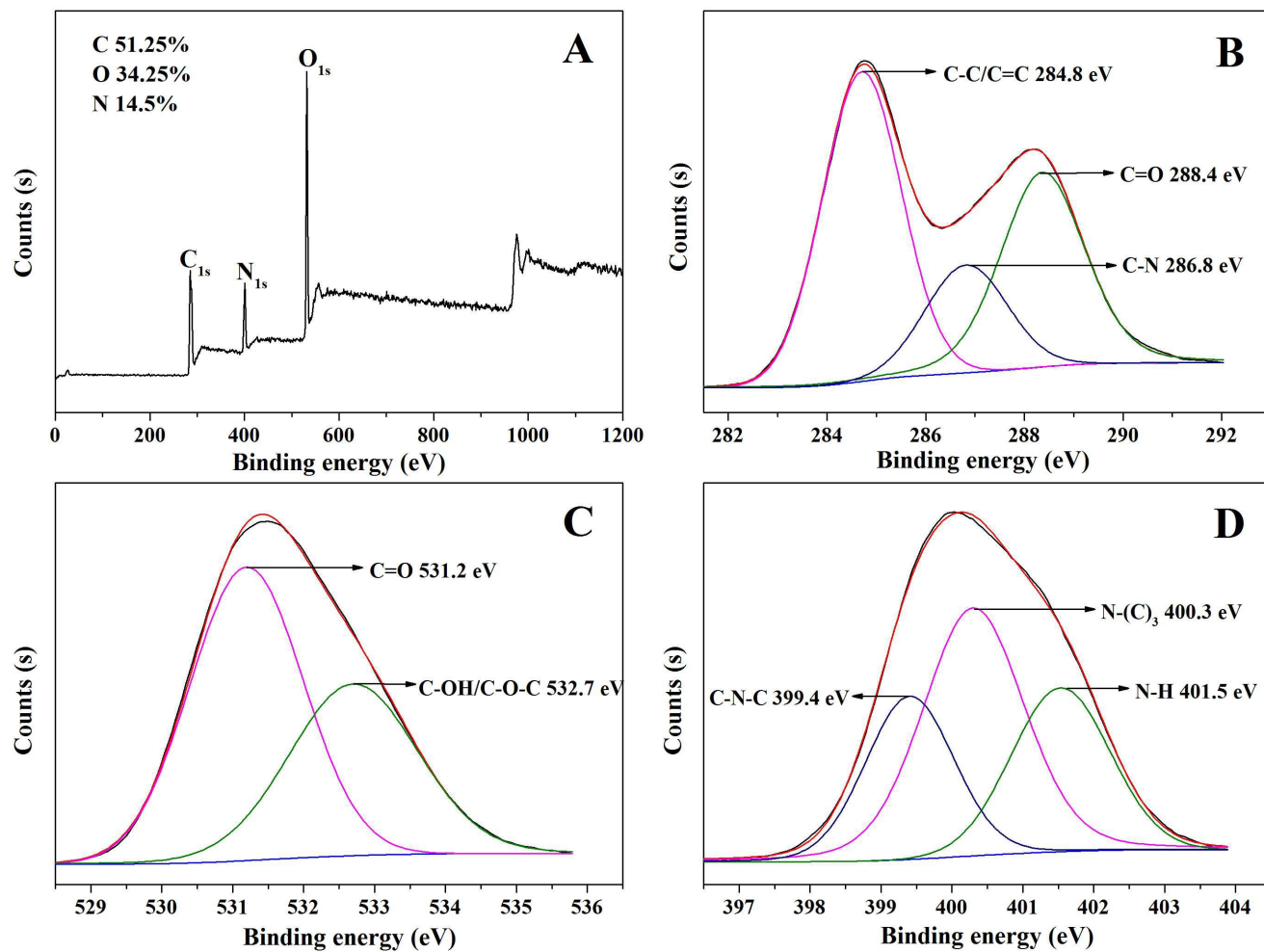


Fig. 3. (A) XPS spectra of the NCDs. (B-D) High-resolution XPS spectra of C1s (B), O1s (C) and N1s (D).

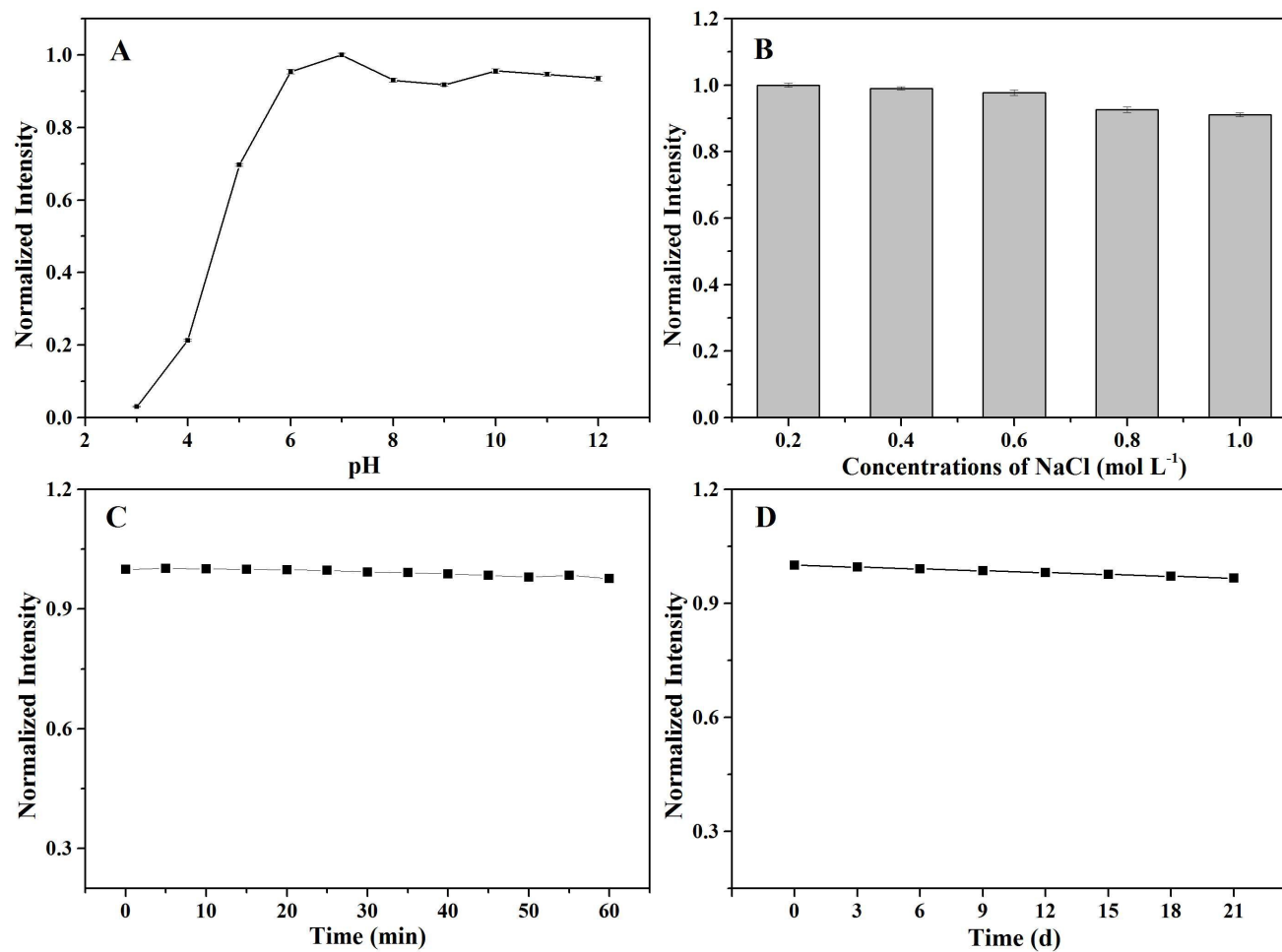


Fig. 4. (A) Normalized fluorescence intensities of NCDs at different pH. (B) Fluorescence response of NCDs in the presence of different concentrations of NaCl. (C) Normalized fluorescence intensities (440nm) of NCDs under the UV illumination of 365 nm at different times. (D) Normalized fluorescence intensities (440nm) of NCDs stored in a refrigerator up to three weeks.

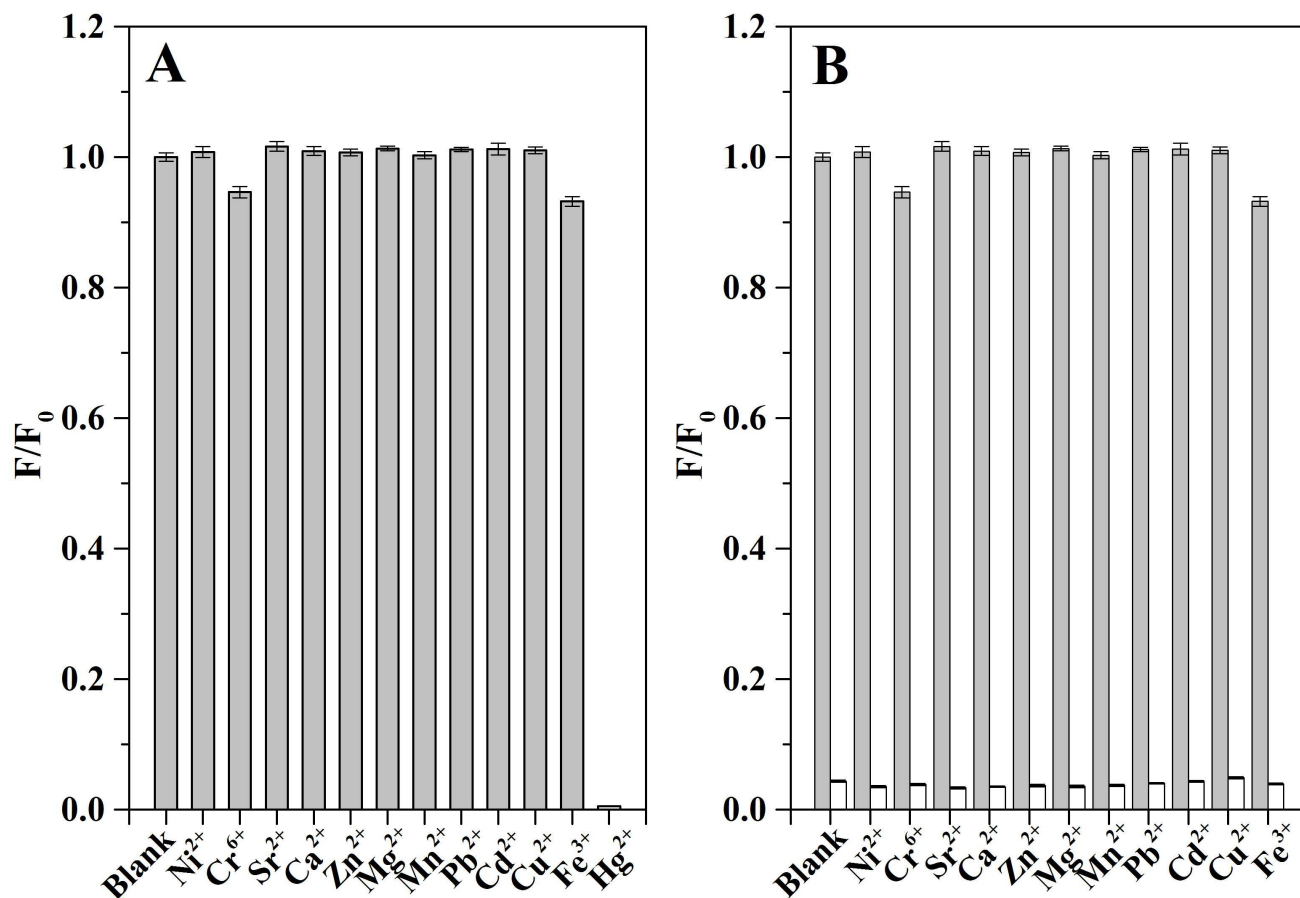


Fig. 5. (A) Fluorescence responses of NCDs to different metal ions under acetate buffer (10 mmol L^{-1} , pH 6.0). The concentration of each metal ion is $20 \text{ }\mu\text{mol L}^{-1}$. F_0 and F correspond to the fluorescence intensities of NCDs at 440 nm excited at 340 nm in the absence and presence of metal ions, respectively. (B) The fluorescence intensities of M+FCDs (M represents any one of metal ions except for Hg^{2+}) solutions before (grey) and after (white) mixing with Hg^{2+} ($10.0 \text{ }\mu\text{mol L}^{-1}$).

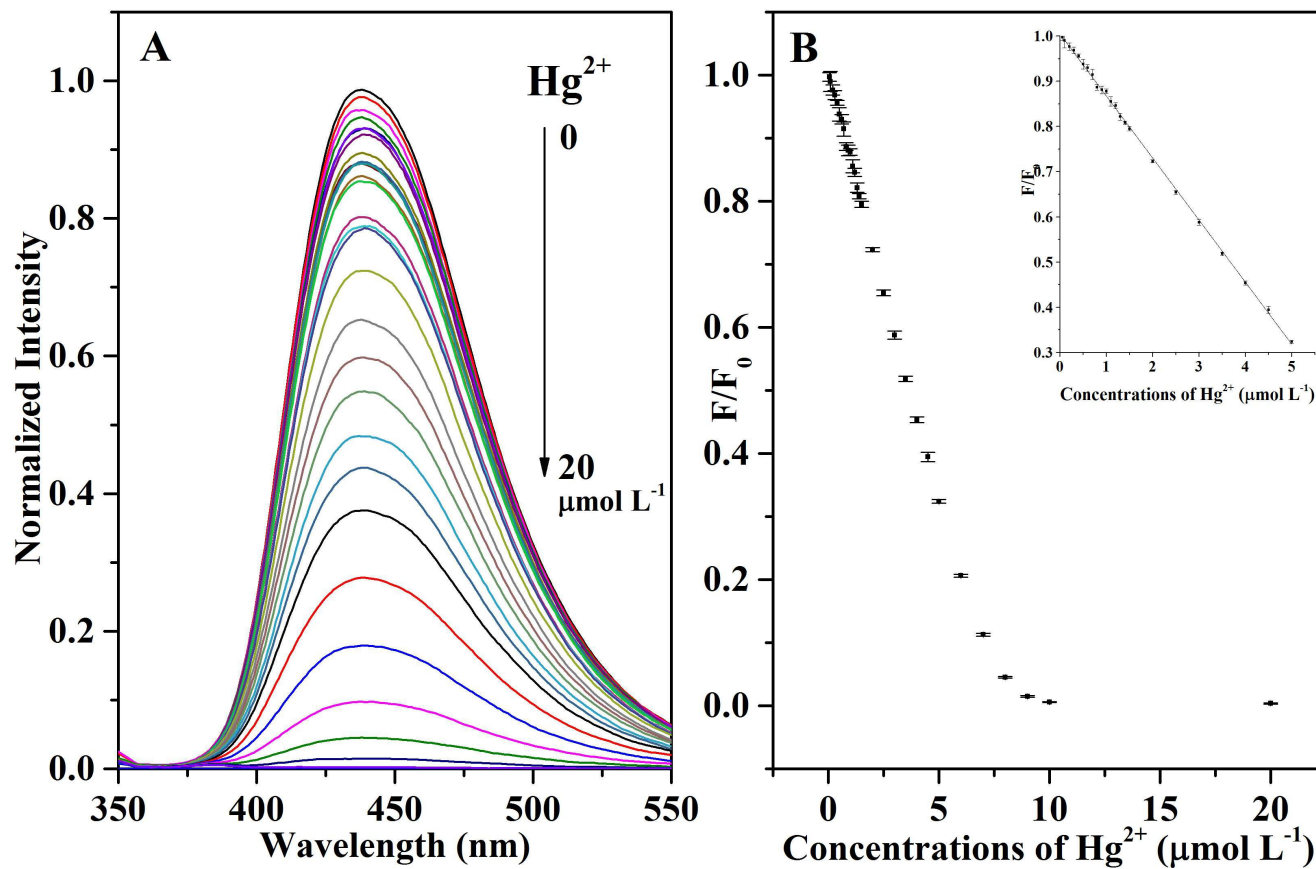


Fig. 6. (A) Emission spectra of NCDs mixed with Hg^{2+} at different concentrations (0 to 20 $\mu\text{mol L}^{-1}$) in acetate buffer (10 mmol L^{-1} , pH 6.0). (B) F/F_0 of NCDs ($\lambda_{\text{ex}}=340$ nm, $\lambda_{\text{em}}=440$ nm) mixed with Hg^{2+} versus the concentrations of Hg^{2+} . The inset plot shows the linear region of the curve ($n=3$).

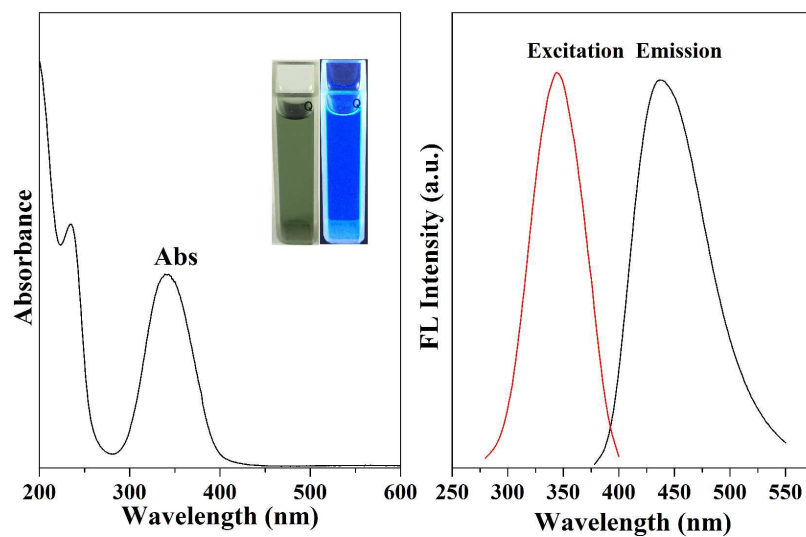
Table 1. Recovery tests of spiked Hg²⁺ in different water samples measured with NCDs and HG-AFS, respectively. (*n*=3)

Samples	Spiked Hg ²⁺ ($\mu\text{mol L}^{-1}$)	NCDs		HG-AFS	
		Measured value ($\mu\text{mol L}^{-1}$)	Recovery (%)	Measured value ($\mu\text{mol L}^{-1}$)	Recovery (%)
Tap water	0.2	0.181 \pm 0.007	90.4	0.196 \pm 0.003	97.9%
	0.4	0.388 \pm 0.008	97.1	0.399 \pm 0.002	99.7%
	1.0	0.982 \pm 0.007	98.2	1.003 \pm 0.004	100.3%
Lake water 1	0.2	0.161 \pm 0.007	81.7	0.196 \pm 0.003	98.0
	0.4	0.332 \pm 0.005	83.1	0.401 \pm 0.002	100.3
	1.0	0.871 \pm 0.004	87.1	1.012 \pm 0.003	101.2
Lake water 2	0.2	0.168 \pm 0.006	84.0	0.197 \pm 0.002	98.2
	0.4	0.344 \pm 0.004	86.1	0.402 \pm 0.001	100.4
	1.0	0.886 \pm 0.008	88.6	1.011 \pm 0.003	101.1

Tap water was sampled from our laboratory. Lake water 1 and 2 were sampled from Jimei Lake and Jingxian Park respectively in Xiamen city, China.

Table 2. Detection limits and linear ranges of different fluorescent probes for Hg²⁺ detection.

Fluorescent probes	Linear range ($\mu\text{mol L}^{-1}$)	Detection limit (nmol L^{-1})	Ref.
Carbon dots	0.0005–0.01	0.23	[7]
Carbon dots	0 – 3	4.2	[20]
Carbon dots	0 – 5	10	[37]
Nitrogen carbon dots	0 – 25	230	[38]
Fluorescent Ag clusters	0.01 – 5	10	[39]
Carbon dots-labeled ODN	0.005 – 0.2	2.6	[40]
N,S/Carbon dots	0 – 40	2×10^3	[41]
NCDs	0.05 – 5	7.3	This work



UV-vis absorption spectrum (left) and fluorescence excitation and emission spectra (right) of NCDs